EARTH AND PLANETARY SCIENCE LETTERS 15 (1972) 367–375. NORTH-HOLLAND PUBLISHING COMPANY
5

SEA FLOOR SPREADING, PROGRESSIVE ALTERATION OF LAYER 2 BASALTS, AND ASSOCIATED CHANGES IN SEISMIC VELOCITIES

Nikolas I. CHRISTENSEN
Department of Geological Sciences and Graduate Program in Geophysics, University of Washington, Seattle, Washington 98195, U.S.A.

and

Matthew H. SALISBURY
Department of Geological Sciences, University of Washington, Seattle, Washington 98195, U.S.A.

Received 3 March 1972
Received version received 25 Mai 1972

Compressional (V_p) and shear (V_s) wave velocities and the dependent elastic constants have been determined by the pulse transmission technique to 10 kb for basalts from six Atlantic sites of the Deep Sea Drilling Project. V_p and V_s are found to vary linearly with density, V_p ranging at 0.5 kb from 4.53 km/sec for the lowest density sample (2.40 g/cm^3) to 6.37 km/sec for the highest (2.92 g/cm^3), while V_s ranges similarly from 2.09 to 3.38 km/sec. This range of V_p is consistent with the wide variability in layer 2 velocities found from refraction studies. Petrographic and X-ray analyses demonstrate that the wide range in densities observed for these basalts is the result of progressive clay alteration and low-grade metamorphism; elastically this can be noted as an increase at 10 kb in dV_p/dP from 0.01 to 0.05 km/sec kb and an increase at 0.5 kb of compressibility from 1.38 to 2.58 Mb^{-3} with decreasing density. Of particular interest, in the ridge traverse of Leg 3 where the basalt ages are well known, density and velocity decrease linearly with age from the ridge crest to the abyssal plain. At least provincially, where uniformity of rock type may be suspected, it may be possible to derive submarine weathering rates and approximate layer 2 ages from careful refraction surveys.

1. Introduction

On the basis of seismic refraction investigations, the oceanic crust has been divided into three layers. The uppermost layer (layer 1) has been known for many years to consist of unconsolidated and semi-consolidated sediments, but prior to the Deep Sea Drilling Project the composition of the seismic layer underlying the sediments (layer 2) was highly debated. Hamilton [1] interpreted layer 2 as being composed of lithifed sediment, while Hess [2] and Dietz [3] postulated a serpentinite composition. Several authors considered layer 2 as igneous in origin [4–7]. The successful recovery of basalt immediately below the sedimentary layer in the Atlantic and Pacific oceans during the Deep Sea Drilling Project has revealed the nature of at least the upper few meters of layer 2.

Compared with the lower oceanic crust (layer 3), compressional wave velocities determined by seismic refraction for layer 2 show considerable variation. Raitt [8] has reported velocities for this layer ranging from 4.12 to 6.32 km/sec. This variability may result from several causes, including differences in the acoustic properties of basalts and interlayering of basalts with sediments. In addition, many problems arise in obtaining velocities and thicknesses of layer 2 from seismic refraction measurements due to the limited distance over which this layer can be observed as a first arrival [8]. It has thus been difficult in the past to separate compositional variability from observational error.

The Deep Sea Drilling Program has provided a remarkable means for examining this variability and its causes in at least the uppermost levels of layer 2. With this objective in mind, we have measured compressional and shear wave velocities to hydrostatic pressures of 10 kb for the basalts obtained from Legs 2, 3, and 4. The results of this study provide velocity-density relationships for layer 2 basalts and explain much of the variation of compressional wave velocities reported for layer 2.

2. Description of specimens and experimental data

A summary of the drilling results for the Atlantic sites from which basalts were recovered in sufficient amounts for this study is given in table 1; more detailed site descriptions may be found in volumes II, III, and IV of the initial reports of the Deep Sea Drilling Project [9–11]. Site locations are shown in fig. 1 with an insert of the magnetic anomalies in the vicinity of the Leg 3 sites [12]. These sites will be of particular interest since they are of varying age within a single province.

Petrography of the basalts included in this study is summarized in table 2. The samples appear to be tholeiitic except for the sample from site 4–23 off Cape Natal which apparently was cored in an alkali basalt sill [11] approximately 260 meters above layer 2. The densities and degrees of alteration, as can be seen from tables 2 and 3, are extremely variable and inversely dependent.

Cores 1.27 cm in diameter and 2.5 to 3.2 cm in length were cut in mutually perpendicular directions from each sample. Bulk densities and velocities of the cores are given in table 3. All velocities were measured at room temperature from water-saturated samples

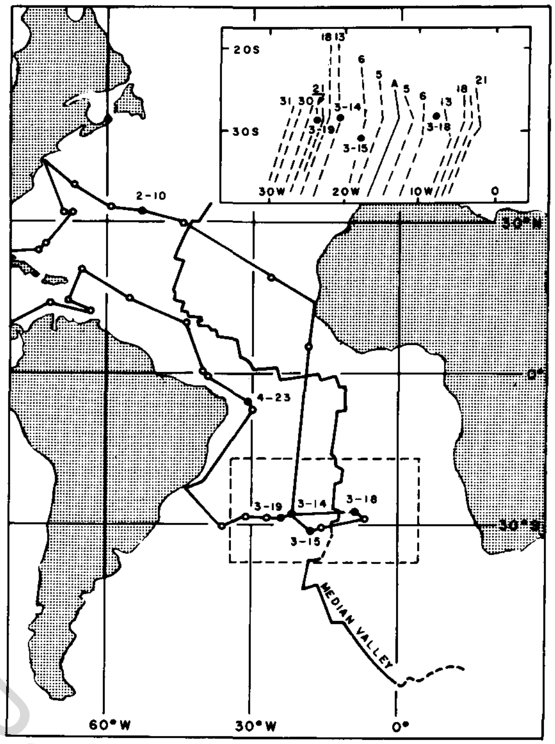

Fig. 1. Leg 2, 3 and 4 site locations. Filled circles indicate sites examined in this study. Magnetic anomaly ages in the vicinity of Leg 3 (insert) are after Dickson et al. [12].

(pore pressure ≪ external pressure). The identification numbers in table 3 give the leg, hole, and core numbers from which the samples were obtained and indicate whether the cores were cut parallel or perpendicular to the site drill-hole.

Table 1
Site summary.

Leg	Site	Latitude	Longitude	Water depth [m]	Sediment thickness [m]	Amount of basalt recovered [m]	Age of oldest sediment [my]
2	10	32° 51.73′N	52° 12.92′W	4697	457	2.75	80
3	14	28° 19.89′S	20° 56.46′W	4346	107	0.60	39 (38*)
3	15	30° 53.38′S	17° 58.99′W	3938	141	0.30	24 (21*)
3	18	27° 58.72′S	08° 00.70′W	4022	178	0.55	26
3	19	28° 32.08′S	23° 40.63′W	4685	141	2.30	49 (53*)
4	23	06° 08.75′S	31° 02.06′W	5085	184	0.47	probable sill

* = anomaly age determination

Table 2
Modal analyses (volume %) (listed in order of decreasing bulk density).

Identification number	Plagioclase	Pyroxene	Olivine	Opaques	Vesicles	Others*	Remarks
3–15–10	32	32	Trace	1	1	34	Fresh porphyritic basalt with subvariolitic to intergranular texture. Alteration minor.
3–18–7	32	1	Trace	1	–	66	Porphyritic basalt with variolitic texture, calcite vein fillings. Alteration to clays moderately developed.
3–14–10	40	1	–	3	–	56	Basalt with variolitic texture, calcite vein fillings. Alteration to clays moderately developed.
2–10–20	25	20	–	5	1	49	Coarse-grained vesicular basalt (subdiabasic). Zeolite and calcite vesicle fillings.
4–23–7	22	10	–	1	2	65	Coarse-grained, highly vesicular basalt with variolitic texture. Pronounced alteration to zeolites and clays.
3–19–12	25	–	–	2	4	69	Porphyritic basalt with recrystallized glass; strongly altered.

* Fine-grained matrix, alteration products and glass.

Table 3
Compressional (P) and shear (S) wave velocities in km/sec.

Identification number	Bulk density	Mode	P = 0.2 kb	P = 0.4 kb	P = 0.6 kb	P = 0.8 kb	P = 1.0 kb	P = 2.0 kb	P = 4.0 kb	P = 6.0 kb	P = 8.0 kb	P = 10.0 kb
3–19–12A ⊥	2.395	P	4.48	4.51	4.54	4.56	4.586	4.674	4.824	4.965	5.085	5.192
B ∥	2.500	P	4.74	4.77	4.80	4.82	4.843	4.930	5.062	5.172	5.279	5.379
Mean	2.448	P	4.61	4.64	4.67	4.69	4.715	4.802	4.943	5.069	5.182	5.286
A ⊥	2.395	S	1.95	2.05	2.13	2.19	2.230	2.374	2.551	2.647	2.698	2.722
B ∥	2.500	S	1.99	2.09	2.16	2.22	2.270	2.423	2.601	2.700	2.756	2.785
Mean	2.448	S	1.97	2.07	2.15	2.21	2.250	2.399	2.576	2.674	2.727	2.753
4–23–7 A ⊥	2.531	P	4.40	4.44	4.47	4.50	4.519	4.607	4.741	4.854	4.946	5.013
B ∥	2.557	P	4.55	4.61	4.64	4.67	4.700	4.795	4.934	5.043	5.142	5.224
C ⊥	2.538	P	4.54	4.58	4.61	4.63	4.651	4.731	4.848	4.948	5.032	5.104
Mean	2.542	P	4.50	4.54	4.57	4.60	4.623	4.711	4.841	4.948	5.040	5.114
A ⊥	2.531	S	2.32	2.35	2.38	2.42	2.443	2.553	2.688	2.775	2.842	2.904
B ∥	2.557	S	2.19	2.23	2.25	2.27	2.284	2.343	2.408	2.440	2.459	2.468
C ⊥	2.538	S	2.20	2.24	2.27	2.29	2.310	2.373	2.442	2.485	2.511	2.530
Mean	2.542	S	2.24	2.27	2.30	2.33	2.346	2.423	2.513	2.567	2.604	2.634
2–10–20A ⊥	2.632	P	4.83	4.89	4.93	4.96	4.985	5.087	5.234	5.355	5.442	5.490
B ∥	2.619	P	4.79	4.84	4.89	4.93	4.963	5.082	5.230	5.355	5.457	5.548
C ⊥	2.611	P	4.75	4.80	4.84	4.87	4.897	4.997	5.151	5.265	5.350	5.417
Mean	2.621	P	4.79	4.84	4.89	4.92	4.948	5.055	5.205	5.325	5.416	5.485
A ⊥	2.632	S	2.32	2.36	2.40	2.44	2.468	2.583	2.712	2.782	2.824	2.842
B ∥	2.619	S	2.17	2.28	2.35	2.40	2.433	2.548	2.644	2.702	2.741	2.766
C ⊥	2.611	S	2.19	2.28	2.33	2.38	2.413	2.520	2.617	2.673	2.719	2.742
Mean	2.621	S	2.23	2.31	2.36	2.41	2.438	2.550	2.658	2.719	2.761	2.783
3–14–10A ⊥	2.762	P	5.52	5.54	5.56	5.57	5.583	5.697	5.792	5.837	5.910	5.943
B ∥	2.780	P	5.73	5.75	5.77	5.78	5.788	5.814	5.855	5.905	5.953	5.988
Mean	2.771	P	5.63	5.65	5.67	5.68	5.686	5.756	5.824	5.871	5.932	5.966
A ⊥	2.762	S	2.91	2.93	2.93	2.97	2.984	3.036	3.087	3.105	3.111	3.112
B ∥	2.780	S	2.94	2.96	2.97	2.98	2.997	3.044	3.106	3.144	3.171	3.183
Mean	2.771	S	2.93	2.95	2.96	2.98	2.991	3.040	3.097	3.125	3.141	3.148
3–18–7 A ⊥	2.819	P	5.87	5.89	5.91	5.92	5.933	5.984	6.053	6.102	6.143	6.168
B ⊥	2.820	P	5.73	5.79	5.82	5.89	5.865	5.935	6.018	6.069	6.108	6.135
Mean	2.820	P	5.80	5.84	5.87	5.91	5.899	5.960	6.036	6.086	6.126	6.152
A ⊥	2.819	S	3.09	3.10	3.12	3.13	3.138	3.174	3.209	3.224	3.235	3.242
B ⊥	2.820	S	3.12	3.13	3.15	3.15	3.163	3.188	3.210	3.220	3.228	3.333
Mean	2.820	S	3.11	3.12	3.14	3.14	3.151	3.181	3.210	3.222	3.232	3.288
3–15–10A ⊥	2.892	P	6.15	6.19	6.22	6.24	6.251	6.310	6.395	6.453	6.501	6.536
B ⊥	2.920	P	6.35	6.36	6.38	6.39	6.396	6.438	6.503	6.551	6.587	6.615
Mean	2.906	P	6.25	6.28	6.30	6.32	6.324	6.374	6.449	6.502	6.544	6.576
A ⊥	2.892	S	3.18	3.21	3.23	3.25	3.270	3.332	3.403	3.446	3.472	3.482
B ⊥	2.920	S	3.35	3.37	3.38	3.39	3.398	3.429	3.456	3.471	3.479	3.482
Mean	2.906	S	3.27	3.29	3.31	3.32	3.334	3.381	3.430	3.459	3.476	3.482

Table 4
Elastic constants calculated from V_p, V_s, and ρ.

Identification number	Pressure [kb]	V_p/V_s	σ	ϕ $[\mathrm{km\,s^{-1}}]^2$	K [Mb]	β $[\mathrm{Mb}^{-1}]$	μ [Mb]	E [Mb]	λ [Mb]
3–19–12	0.4	2.24	0.38	15.8	0.39	2.58	0.10	0.29	0.32
	1.0	2.10	0.35	15.5	0.38	2.64	0.12	0.34	0.30
	2.0	2.00	0.33	15.3	0.38	2.65	0.14	0.38	0.28
	6.0	1.90	0.31	16.0	0.40	2.51	0.18	0.46	0.28
	10.0	1.92	0.31	17.6	0.44	2.27	0.19	0.49	0.32
4–23–7	0.4	2.00	0.33	13.7	0.35	2.86	0.13	0.35	0.26
	1.0	1.97	0.33	14.0	0.36	2.80	0.14	0.37	0.26
	2.0	1.94	0.32	14.3	0.37	2.73	0.15	0.39	0.27
	6.0	1.93	0.32	15.5	0.40	2.49	0.17	0.44	0.29
	10.0	1.94	0.32	16.6	0.43	2.31	0.18	0.47	0.31
2–10–20	0.4	2.10	0.35	16.3	0.43	2.34	0.14	0.38	0.33
	1.0	2.03	0.34	16.5	0.43	2.30	0.16	0.42	0.33
	2.0	1.98	0.33	16.8	0.44	2.26	0.17	0.45	0.33
	6.0	1.96	0.32	18.3	0.49	2.05	0.19	0.52	0.36
	10.0	1.97	0.33	19.5	0.52	1.92	0.20	0.54	0.39
3–14–10	0.4	1.92	0.31	20.3	0.56	1.78	0.24	0.63	0.40
	1.0	1.90	0.31	20.4	0.57	1.77	0.25	0.65	0.40
	2.0	1.89	0.31	20.8	0.58	1.73	0.26	0.67	0.41
	6.0	1.88	0.30	21.3	0.60	1.68	0.27	0.71	0.42
	10.0	1.90	0.31	22.1	0.62	1.60	0.28	0.72	0.44
3–18–7	0.4	1.87	0.30	21.1	0.60	1.68	0.27	0.71	0.41
	1.0	1.87	0.30	21.5	0.61	1.64	0.28	0.73	0.42
	2.0	1.87	0.30	22.0	0.62	1.61	0.29	0.74	0.43
	6.0	1.89	0.31	23.1	0.66	1.52	0.29	0.77	0.46
	10.0	1.87	0.30	23.2	0.66	1.51	0.31	0.80	0.46
3–15–10	0.4	1.91	0.31	25.0	0.73	1.38	0.31	0.82	0.52
	1.0	1.90	0.31	25.1	0.73	1.37	0.32	0.85	0.52
	2.0	1.89	0.30	25.3	0.74	1.35	0.33	0.87	0.52
	6.0	1.88	0.30	26.2	0.77	1.30	0.35	0.91	0.53
	10.0	1.89	0.31	26.9	0.79	1.27	0.35	0.92	0.55

Travel times through the specimens were determined by the pulse transmission technique [13, 14]. 2MHz barium titanate and AC-cut quartz transducers were used to generate and receive compressional and shear waves respectively. Since the technique is generally considered accurate to $\frac{1}{2}$% for compressional and 1% for shear wave velocities, the reporting of velocity to the fourth place in table 3 is meant to convey only slope information, not accuracy. Pressure was measured by determining the change in electrical resistance of a calibrated manganin coil immersed in the pressure medium. The pressure system utilized a standard two stage intensifier which is capable of producing hydrostatic pressures in excess of 10 kb in a cylindrical cavity of 300 cm^3.

The ratio of compressional to shear velocity (V_p/V_s), Poisson's ratio (σ), the seismic parameter (ϕ), the bulk modulus (K), compressibility (β), the shear modulus (μ), Young's modulus (E), and Lamé's constant (λ) calculated at selected pressures for each rock are given in table 4. The equations relating these constants to velocities and density are summarized by

Birch [15]. Mean velocities and densities used in the calculations were corrected for dimension changes at high pressures using an iterative routine and the dynamically determined compressibilities.

3. Velocity–density relations

Of particular significance is the wide range of densities (2.395 to 2.920 g/cm^3) found for the layer 2 basalts. Examination of table 3 shows that cores from basalts with low mean densities are somewhat more variable in density than the high density basalts. This appears to result from alteration and perhaps the vesicularity of the low density basalts. Though the velocity variations among cores from a given site are generally small, those variations noted tend to be density-dependent. Thus the range in velocities reported for each site is most likely due to inhomogeneity rather than anisotropy produced by preferred mineral orientation.

The compressional and shear wave velocities show an excellent correlation with bulk density. This is illustrated in figs. 2 and 3, where compressional and shear wave velocities at 0.5 kb (an approximate pressure for layer 2) are plotted against bulk densities. Least-square regression line parameters at selected pressures of density on velocity and velocity on density are given in table 5. The slope of the 10 kb velocity on density regression line compares favorably with Birch's determination of 2.92 km sec^{-1}/g cm^{-3} for rocks of mean atomic weight 22. This excellent fit and the high cor-

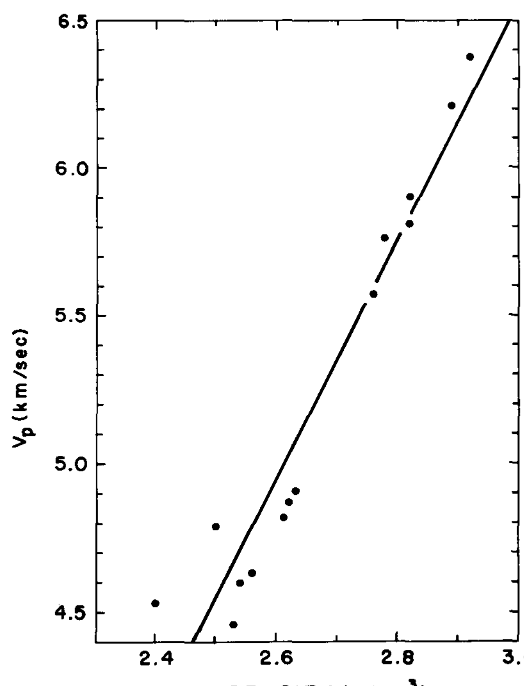

Fig. 2. Compressional velocity (V_p) vs. density (ρ) for Legs 2, 3, and 4 submarine basalts at 0.5 kb.

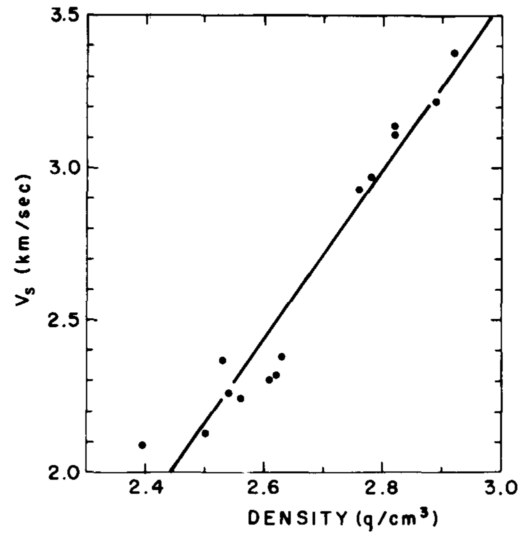

Fig. 3. Shear velocity (V_s) vs. density (ρ) for Legs 2, 3 and 4 submarine basalts 0.5 kb.

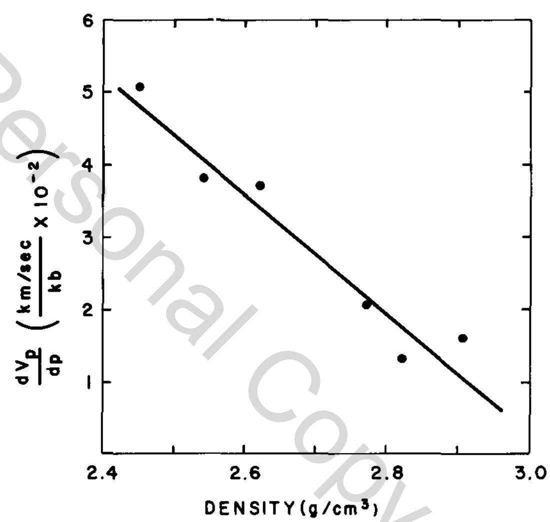

Fig. 4. dV_p/dP vs. ρ for Legs 2, 3 and 4 submarine basalts at 10 kb.

Table 5
Regression line parameters.

Pressure [kb]	n	a [km s^{-1}]	b $\left[\frac{\text{km s}^{-1}}{\text{g cm}^{-3}}\right]$	$S_{(V,\rho)}$ [km s^{-1}]	r	r^2 [%]
			$V_p = a + b\rho$			
0.5	14	−5.45	4.00	0.17	0.96	93
1.0	14	−5.23	3.94	0.16	0.97	93
2.0	14	−4.89	3.84	0.15	0.97	94
6.0	14	−3.66	3.45	0.15	0.96	93
10.0	14	−2.65	3.12	0.16	0.95	91
			$V_s = a + b\rho$			
0.5	14	−4.76	2.77	0.11	0.97	94
1.0	14	−4.16	2.57	0.10	0.97	94
2.0	14	−3.52	2.36	0.11	0.96	92
6.0	14	−2.30	1.95	0.13	0.92	84
10.0	14	−1.96	1.85	0.15	0.89	80

Pressure [kb]	n	a [g cm^{-3}]	b $\left[\frac{\text{g cm}^{-3}}{\text{km s}^{-1}}\right]$	$S_{(\rho,V)}$ [g cm^{-3}]	r	r^2 [%]
			$\rho = a + bV_p$			
0.5	14	1.46	0.232	0.042	0.96	93
1.0	14	1.42	0.237	0.020	0.97	93
2.0	14	1.36	0.244	0.039	0.97	94
6.0	14	1.17	0.269	0.041	0.96	93
10.0	14	1.02	0.290	0.048	0.95	91
			$\rho = a + bV_s$			
0.5	14	1.78	0.339	0.038	0.97	94
1.0	14	1.69	0.364	0.039	0.97	94
2.0	14	1.58	0.391	0.043	0.96	92
6.0	14	1.41	0.430	0.062	0.92	84
10.0	14	1.39	0.431	0.070	0.89	80

n = number of data points,
$S_{(V,\rho)}$ = standard error of estimate of V on ρ,
$S_{(\rho,V)}$ = standard error of estimate of ρ on V,
r = correlation coefficient,
r^2 = coefficient of determination.

relation coefficients noted in table 5 appear to be characteristic of basalts retrieved in the Deep Sea Drilling Project. Dredged basalts typically display lower correlation coefficients and a notable departure from the m = 22 solution [16].

At pressures above a few kilobars where the effects of crack porosity are largely eliminated [15], the change of velocity with pressure, dV_p/dP, also correlates well with density as is illustrated for compressional wave velocities in fig. 4. The lower density basalts have the higher pressure derivatives. Again this most likely results from the progressive alteration of the basalts.

4. Discussion

The Deep Sea Drilling Program, by sampling of the uppermost levels of layer 2 has provided direct means for verification of velocities obtained by surface refraction techniques and for interpreting these velocities in terms of petrology. The velocities obtained in this study display the same range and extreme variability that have long been noted in refraction data for layer 2. From an examination of figs. 2 and 3 and the regression line parameters of table 5, it can be seen that V_p and V_s vary linearly with density; the degree of fit is exceptional. From an examination of thin sections, it is clear that the densities of the basalts depend in turn on the degrees of clay alteration and low grade metamorphism in the samples, both processes operating to lower density and thus seismic velocity. It is therefore suggested that the range of velocities obtained for the upper levels of layer 2 can be attributed to varying degrees of alteration, though this need not be the only explanation. It should be noted, that no correlation was found between the degree of alteration and sample depth within layer 2.

Though additional study of JOIDES cores is necessary in order to reach firm conclusions, there is, as can be seen in fig. 5, a strong suggestion from the Leg 3 cores that the seismic velocity and density of at least the uppermost levels of layer 2 systematically decrease with age from the Mid-Atlantic Ridge crest to the abyssal plains. Though this conclusions may well be disproven by the availability of more complete data in the future, it appears at present to be at least qualitatively correct.

After generation of basalt at the ridge crest, weathering processes and low grade metamorphism should commence in at least the uppermost basalts of layer 2, their effects becoming increasingly profound with age. Petrographic examination of the basalts included in this study reveals precisely this relation. The basalt from the youngest site of Leg 3, site 15, has the highest seismic velocity and is the most dense, least altered specimen examined. With increasing age, the specimens display increasing alteration to clays and the initial

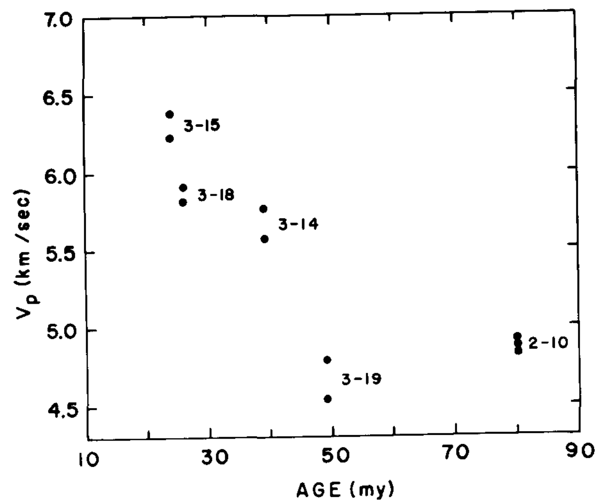

Fig. 5. Compressional velocity (V_p) vs. age for Legs 2 and 3 submarine at 0.5 kb (data from the basalt of Leg 4, site 23, retrieved from a sill of uncertain age, are omitted).

stages of low grade metamorphism; these processes are accompanied by a decrease in density. The most profoundly altered and least dense basalt from Leg 3 (recovered from site 19) was the oldest of the traverse. In support of this Hart [17] and Hekinian [18] have noted systematic chemical changes in dredged basalts with age. The oxides of calcium, silicon, and magnesium decrease with age, whereas the oxides of titanium, potassium and phosphorus, plus total iron and water increase. Based upon comparisons of fresh ridge basalts with weathered ridge basalts, Hart concluded that these trends which both authors ascribe to progressive submarine weathering, must produce a net decrease in density with time. On the basis of chemical data alone, he calculated this decrease to be

$$\frac{\Delta\rho}{\Delta t} = 0.38 \times 10^{-2}\ \mathrm{g/cm^3\ my} = 0.15\%/\mathrm{my}$$

for the period 0 to 18 my. Fitting a least squares regression line of age on density allows an independent evaluation of submarine weathering rates from direct density measurements for the interval 24 to 80 my equal to

$$\frac{\Delta\rho}{\Delta t} = 0.52 \times 10^{-2}\ \mathrm{g/cm^3\ my} = 0.18\%/\mathrm{my}$$

in excellent agreement with Hart's findings. These weathering rates are non-trivial; after 80 my a submarine basalt has lost 15% of its initial mass.

The laboratory determined decreases in seismic velocity and density with age are in qualitative agreement with the findings of Le Pichon et al. [19] in the North Atlantic that compressional wave velocities for layer 2 tend to decrease with increasing water depth. Since the depth of the ridge province generally increases with distance from the crest and thus with age, the velocity decreases with age. Curiously, compressional wave velocities appear to rise to over 5 km/sec at distances of approximately 600 km from the ridge crest. The somewhat elevated determined in the laboratory for cores from site 10, the most distant site from the ridge, may reflect this rise. A similar decrease in compressional wave velocity with age, together with a noticeable rise in velocity under the abyssal plain is clearly seen in the refraction data of Raitt [20] near the East Pacific Rise (sites c-17 through c-22). It may thus be possible in a given lithologic province to derive submarine weathering rates and approximate ages from careful refraction surveys.

Acknowledgements

M. Mulcahey, R. McConaghy, and R. Carlson provided technical assistance for the study. Samples were supplied through the assistance of the National Science Foundation. The research was supported by National Science Foundation grant GA-20317.

References

[1] E.L. Hamilton, On the thickness and consolidation of deep-sea sediments, Bull. Geol. Soc. Am. 70 (1959) 1399.

[2] H.H. Hess, History of ocean basins, in: A.E.J. Engel, H.L. James and B.F. Leonard (eds.), Petrologic Studies – Buddington Vol. Geol. Soc. Am., N.Y. (1962) 599.

[3] R.S. Dietz, Alpine serpentines as oceanic rind fragments, Bull. Geol. Soc. Am. 74 (1963) 947.

[4] J. Ewing and M. Ewing, Seismic refraction profiles in the Atlantic Ocean basins, Mediterranean Sea, Mid-Atlantic Ridge, and Norwegian Sea, Bull. Geol. Soc. Am. 70 (1959) 291.

[5] A.E.J. Engel, C.G. Engel and R.G. Havens, Chemical characteristics of oceanic basalts and the upper mantle, Bull. Geol. Soc. Am. 76 (1965) 719.

[6] J.R. Cann, Geological processes at mid-ocean ridge crests, Geophys. J.R. astr. Soc. 15 (1968) 331.

[7] N.I. Christensen, Composition and evolution of the oceanic crust, Marine Geol. 8 (1970) 139.

[8] R.W. Raitt, The crustal rocks, in: M.N. Hill (ed.), The Sea 3, Wiley, N.Y. (1963) 85.

[9] M.N.A. Peterson, N.T. Edgar, M. Cita, S. Gartner, Jr., R. Goll, C. Nigrini and C. Von der Borch, Initial reports of the Deep Sea Drilling Project, Volume II (U.S. Government Printing Office, Washington, 1970).

[10] A.E. Maxwell, R.P. Von Herzon, J.E. Andrews, R.E. Boyce, E.D. Milow, K.J. Hsu, S.F. Percival and T. Saito, Initial reports of the Deep Sea Drilling Project, Volume III (U.S. Government Printing Office, Washington, 1970).

[11] R.G. Bader, R.D. Gerard, W.E. Benson, H.M. Bolli, W.W. Hay, W.T. Rothwell, Jr., M.H. Ruef, W.R. Riedel and F.L. Sayles, Initial reports of the Deep Sea Drilling Project, Volume IV (U.S. Government Printing Office, Washington, 1970).

[12] G.O. Dickson, W.C. Pitman, III and J.R. Heirtzler, Magnetic anomalies in the South Atlantic and ocean floor spreading, J. Geophys. Res. 76 (1968) 2087.

[13] F. Birch, The velocity of compressional waves in rocks to 10 kb, 1, J. Geophys. Res. 65 (1960) 1083.

[14] G. Simmons, Velocity of shear waves in rocks to kb, 1, J. Geophys. Res. 69 (1964) 1123.

[15] F. Birch, The velocity of compressional waves in rocks to 10 kb, 2, J. Geophys. Res. 66 (1961) 2199.

[16] N.I. Christensen and G.H. Shaw, Elasticity of mafic rocks from the Mid-Atlantic Ridge, Geophys. J.R. astr. 20 (1970) 271.

[17] R. Hart, Chemical exchange between sea water and deep ocean basalts, Earth Planet. Sci. Letters 9 (1970) 269.

[18] R. Hekinian, Chemical and mineralogical differences between abyssal hill basalts and ridge tholeiites in the eastern Pacific Ocean, Marine Geology 11 (1971) 77.

[19] X. Le Pichon, R.E. Houtz, C.L. Drake and J.E. Nafe, Crustal structure of mid-ocean ridges, 1. Seismic refraction measurements, J. Geophys. Res. 70 (1965) 319.

[20] R.W. Raitt, Seismic refraction studies of the Pacific ocean basin, 1. Crustal thickness of the central equatorial Pacific, Bull. Geol. Soc. Am. 67 (1956) 1623.